A Single Molecule Level Study of the Temperature Dependent Kinetics for the Formation of Metal Porphyrin Monolayers on Au(111) from Solution

(JACS, 2014, 136, 2142–2148)

Ashish Bhattarai, Ursula Mazur*, and K W Hipps*

Department of Chemistry

Washington State University

Pullman, WA 99164-4630

hipps@wsu.edu

ABSTRACT

Scanning tunneling microscopy was used to make the first molecular scale measurements of the temperature dependence of composition of an adlayer at the solution-solid interface. We conclusively demonstrate that metal porphyrins adsorb very strongly on Au(111) at the solution solid interface such that the monolayer composition is entirely kinetically controlled below about 100 °C. The barrier for desorption is so great in fact that a temperature of 135 °C is required to induce desorption over a period of hours. Moreover, cobalt(II) octaethylporphyrin (CoOEP) and NiOEP desorb at different rates from different sites on the surface. We have measured the rate constant for desorption of CoOEP into phenyloctane to be 6.7×10^{-5} /s at 135 °C. Based on these measurements an upper bound can be set for the desorption rate of NiOEP into phenyloctane as 6.7×10^{-4} /s at 135 °C. For solutions of the order of 100 μM in NiOEP or CoOEP, a dense monolayer is formed within seconds, the adsorption rate constants fall within 40% of each other. The structure of NiOEP and CoOEP monolayers are essentially identical and the molecular spacing for both can be described by A = 1.42±0.02 nm, B = 1.32±0.02 nm, and α = 57º±2º. The solubility of CoOEP and NiOEP in phenyloctane at room temperature was measured to be 0.228 g/L and 0.319 g/L, respectively.

INTRODUCTION

The solution-solid interface is of growing importance to technology. While it has always been critical for processes such as catalysis,[1] spin casting,[2] lubrication and wear,[3-5] and crystallization,[6-8] new demanding applications are appearing. A particularly contemporary example is ink-jet printing of organic electronic components[9-12]. In order to advance these technologies, science must provide an ever increasing understanding of the fundamental processes that occur at the solution-solid boundary.

Until the late 1980's all molecular scale studies of the solid/solution interface were ex situ -- surfaces were exposed to solution, the surface was dried (often put into ultra high vacuum) and then studied. With the advent of the scanning tunneling microscope (STM) it became possible to make molecular and even atomic scale measurements at the solution-solid interface at room temperature. Because of the STM, there has been a dramatic increase in our understanding of molecular process at the solution-solid interface at room temperature. As wonderful as these studies are, they are limited. They probe only a very narrow range of the possible processes but completely ignore what happens when the solution is hotter or colder than room temperature. The ability to see molecules ordering and re-ordering on a surface at different temperatures provides access to new materials, phases, reaction rates, reaction mechanisms, and the kinetics and thermodynamics of these surface processes. Studying the relative distribution and structure of bimolecular phases as a function of temperature allows one to determine relative adsorption energies and entropies. Temperature dependent imaging of film growth allows one to find the ideal temperature and time for a given commercial process. Unlike the case of STM in vacuum, where variable temperature studies abound, there have only been a handful of variable temperature STM studies at the solution-solid interface. [13-25] There are both conceptual and practical reasons why this has occurred. Conceptually, it was commonly believed that non-

covalent ordering at the solution-solid interface is a dynamic process. It was thought that molecule level imaging of physisorbed species from solution was a marginal thing at room temperature because the thermal energy was close to the ordering and/or desorption energy. There is now evidence that STM can be used to image well defined structures at the solid-solution interface at elevated temperatures. [14,19,20,23] Detailed STM studies of surface structures and chemical processes at the solution-solid interface as a function of temperature are just becoming available. [14,23]

In this report we use solution phase STM to investigate the temperature dependence of the rate constants that determine the formation of an ordered monolayer of cobalt(II) octaethylporphyrin (CoOEP) on Au(111) when deposited from a sub-saturation solution in phenyloctane. It is critical to note here that these studies are occurring at the unsaturated solution-solid interface, not just the liquid-solid interface. There have been numerous studies of porphyrins adsorbed on metal or HOPG surfaces from organic solvents, and then studied in aqueous electrochemical environments.[26-28] In aqueous environments the porphyrins studied here and by Itaya are totally insoluble. Thus, there is no possibility of desorption from the surface unless the chemical nature or oxidation state of the porphyrin is changed during the electrochemical process.

In order to study the solution-surface equilibrium, we will use the replacement of CoOEP with NiOEP as a tracer for the desorption process. Thus, we will focus on the kinetics and process of adsorption and desorption of these two metal porphyrins on Au(111). Prior to this study, the porphyrins and their close relative, the phthalocyanines, were extensively investigated as adsorbates on metal surfaces in UHV. [29-33] Mixtures of cobalt and nickel complexes have also been studies in UHV [34,35] and it is now well known that they can be easily differentiated in the STM image. There have also been a number of reports on porphyrins or phthalocyanines

adsorbed on Au and HOPG from solution at room temperature. [20,36-44] Mixtures of porphyrins and phthalocyanines adsorbed from solution have been studied on HOPG at room temperature, with the most relevant reports being those of Miyake and co-workers. [45-47]

In their early reports, Miyake and co-workers measured the ratio of metallated porphyrins and free base porphyrin both on the HOPG surface and in solution at room temperature. They found a non-linear relationship between the solution and surface concentrations. They assumed equilibrium between the surface and solution and used the concentration variation to derive the difference in free energies of adsorption of the metallated and free porphyrins, they called the resulting value $\Delta\Delta G$. [45,46] In 2008, they performed a similar experiment with a Zn porphyrins complex and free base, and also found a non linear relationship between fraction in solution and fraction on the surface of HOPG. In this paper, however, they realized that the assumption of equilibrium was not justified by any data, and they refrained from associating the preferential adsorption with a $\Delta\Delta G$ value. They clearly stated that both kinetics and thermodynamics could be playing a role and that kinetics might be dominating.

Here we will consider the solution phase adsorption of two very similar metallated porphyrins on to Au(111). At room temperature, the adsorptive formation of a monolayer occurs very quickly and is consistent with either similar rates of adsorption or similar free energies of adsorption, or both. By observing the detailed atomic distribution of NiOEP and CoOEP on the surface with time, we find that the concentration of the monolayer is entirely controlled by kinetics. We will show that the desorption rate is almost non-existent at room temperature, and even at 135°C the rate is much slower than for many covalently bound thiols. The temperature dependent experiments reported here make it possible to conclusively show that non-covalent interactions can lead to extremely tight binding of adsorbates at the solution-solid interface.

EXPERIMENTAL SECTION

2,3,7,8,12,13,17,18-Octaethyl-21H,23H-porphine cobalt(II) [CoOEP] and 2,3,7,8,12,13,17,18-Octaethyl-21H,23H-porphine nickel(II) [NiOEP] were purchased from Aldrich and Frontier Scientific, respectively. Phenyloctane (98%) was purchased variously from Aldrich, Alfa Aesar, and Fisher Scientific. All the phenyloctane purchased from the above three companies was subjected to further purification. UV-vis spectra of solutions of CoOEP in undistilled phenyloctane provided as above had two Soret bands at 392 nm and 420 nm instead of a single expected 392 nm band. To get rid of the impurity complexing with CoOEP, phenyloctane was distilled over Al_2O_3 (90% Al_2O_3, 9% H_2O; Alfa products). After several distillations the UV-vis spectra of CoOEP in this solvent indicated that the impurity had been reduced to less than 10 ppm.

UV-vis studies were carried out using a Perkin-Elmer model 330 spectrophotometer with 0.1578 cm path length cuvettes. UV-visible spectroscopy on saturated and filtered solutions of porphyrins in phenyloctane was used to determine solubility at room temperature. The measured solubility of CoOEP in phenyloctane was 3.9×10^{-4} M or 0.228 g/L and that of NiOEP was 5.4×10^{-4} M or 0.319 g/L. The highest concentrations solution used in these experiments was 1.2×10^{-4} M and most were less than 1.1×10^{-4} M.

Au(111) substrates were prepared by epitaxial growth of Au on mica using vapor deposition technique. Au (99.999%) and mica were purchased from Cerac Inc. and Ted Pella Inc. ,respectively. Freshly made Au substrates were hydrogen flame annealed and imaged under STM to ensure that surface reconstruction lines could be seen. Samples were deposited only on Au substrates which had distinct reconstruction lines as observed in the STM images. STM images were recorded using a Molecular Imaging (now Agilent) Pico 5 STM equipped with a scanner capable of imaging a maximum area of 1 μm^2 and having an overall current sensitivity

of 1 nA/V. The Agilent environmental chamber was used for all experiments and an argon atmosphere was maintained. STM tips were primarily prepared by cutting and sometimes (about 15%) electrochemically etching the $Pt_{0.8}Ir_{0.2}$ wire bought from California Fine Wire Company. The best etched and cut tips gave similar results but the cutting process yielded more high quality images faster. Images were typically obtained in constant current mode at a sample potential of -0.7 V and a tunneling current of 20 pA. Images of sizes ranging from 20 x 20 nm^2 to 40 x 40 nm^2 were collected at a scan rate of 4.7 lines/sec, giving a total image time of just under 2 min. Images larger than 40 x 40 nm^2 were scanned at a slower scan rate of 3.3 to 3.9 lines/sec, giving a total image time of roughly 2.5 min. The temperature of the sample was controlled by a variable-temperature hot stage using a Lakeshore 330 auto-tuning temperature controller. The Agilent supplied environmental chamber was purged with 99.996% Ar at all times. Before imaging, samples were allowed to sit for 30 minutes to an hour inside the environmental chamber purged with Ar at 2.5 standard cubic feet per hour (scfh). During imaging, Ar was continuously purged at 0.5 scfh.

Solutions of CoOEP and NiOEP were prepared by dissolving sufficient amount of the respective compounds in phenyloctane. Solution concentrations of $1.2x10^{-4}$ M CoOEP and $1.1x10^{-4}$ M NiOEP were prepared separately. The same stock solutions were used for all the experiments performed by STM. A custom made solution cell sample holder was used to accommodate large volumes of solution in contact with the Au surface (up to 100 µL sample). Large volumes of solution with low surface area were crucial to minimize evaporation during multiple heating operations on the same sample at 135 ^{0}C.

During the sample heating process for the kinetic experiments, the temperature of the sample was ramped from room temperature at a rate of 5 ^{0}C per minute, allowing the sample to reach 135 ^{0}C in 30 min. The sample then was held at 135 ^{0}C for the desired time period. After

the desired period at 135 ^{0}C, samples were allowed to cool down to room temperature by turning the heater off and were then allowed to equilibrate for at least 90 minutes prior to recording any images. All STM images were background subtracted using SPIP image processing software.

RESULTS AND DISCUSSION

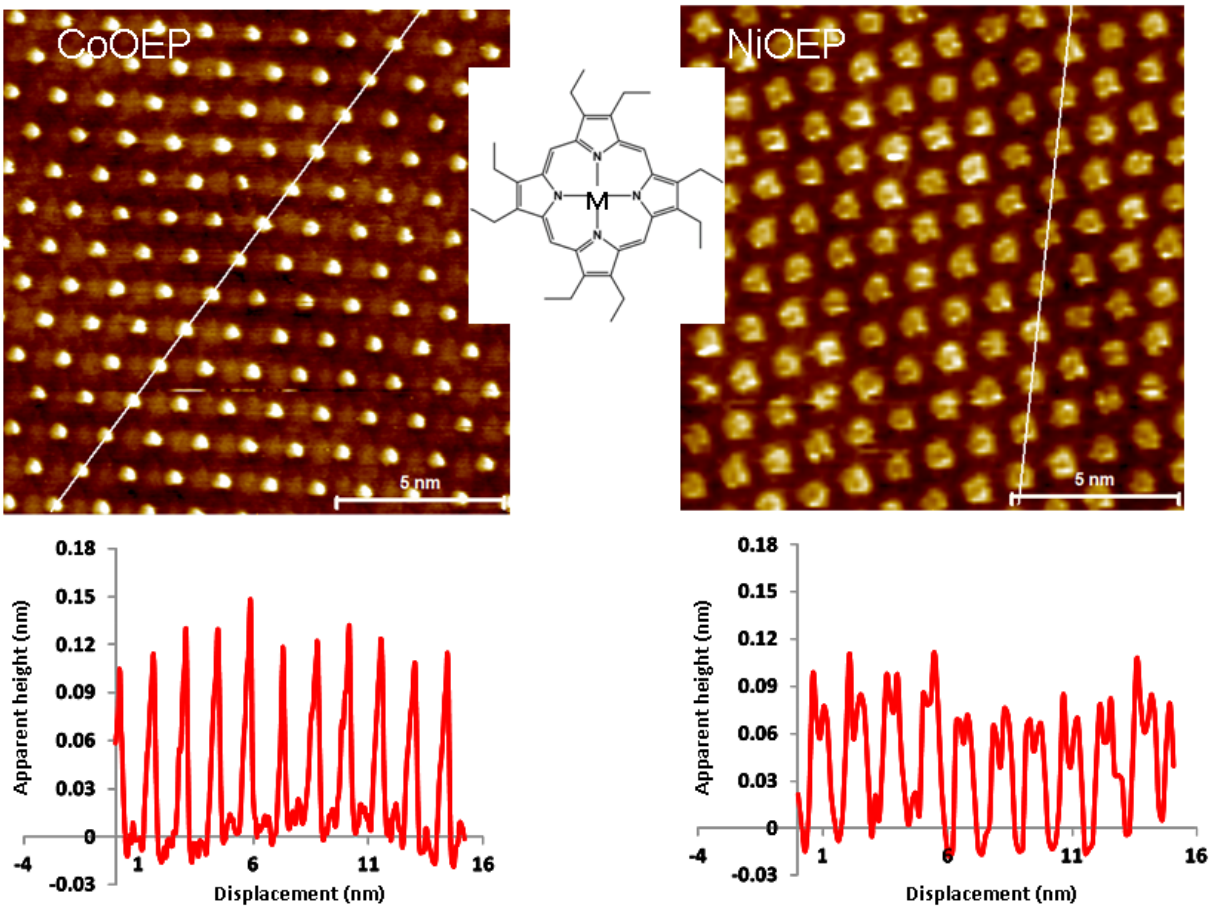

Figure 1: Constant current STM images of the interface formed between a solution of a pure MOEP complex in phenyloctane and the Au(111) surface. The left image is of CoOEP and the right is of NiOEP. Cross sectional apparent height data is also shown.

Figure 1 contrasts the constant current STM images seen from a monolayer of CoOEP (120 μM) and of NiOEP (110 μM) on Au(111) formed at the solution-solid interface with a solution of the appropriate porphyrins in phenyl octane at 25°C. Also shown in the figure are cross

sections and the structure of the complex. Note that the solutions had been deoxygenated and that all data was acquired under Argon. As is expected from studies in UHV, [35,48] the cobalt center of the CoOEP appears very high at the bias voltage used, while the nickel atom appears as a depression. It should be noted that the localization of the central peak (or depression) depends upon tip sharpness, so the CoOEP sometimes appears as a wider bright region. The NiOEP always appears shorter (dimmer) than CoOEP for all tips used.

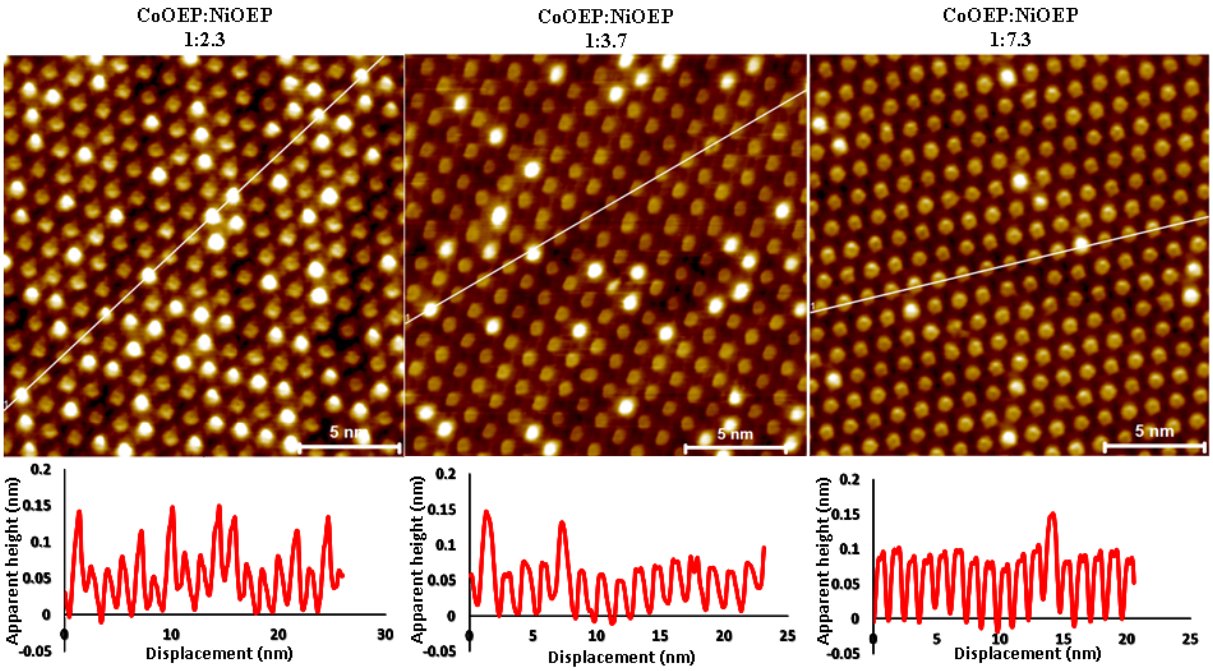

Figure 2. Effect of relative amounts of CoOEP to NiOEP in solution in contact with Au(111) on the constant current STM images obtained. STM images were obtained under set point conditions of -0.7 V sample bias and 20 pA.

When a Au(111) surface is exposed to a solution containing a mixture of CoOEP and NiOEP in phenyloctane, the monolayer formed contains a mixture of the two species. For example, Figure 2 contrasts the STM images seen with three different relative concentrations at 25°C. As can bee seen from both the images and the cross sections, NiOEP is easily distinguished from CoOEP, and the surface concentration of CoOEP diminishes as its relative solution concentration decreases. The experiments depicted in Figure 2 were repeated for five different concentrations and many images were collected in order to assure statistical

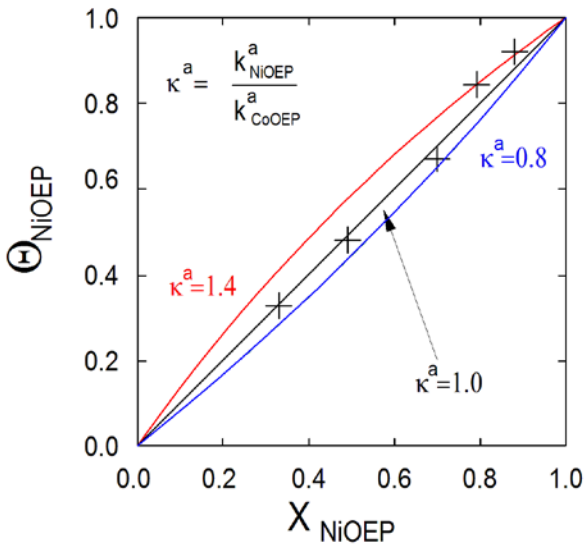

Figure 3: Mole fraction of NiOEP on Au(111) versus in solution at 25°C.

significance. The ratio of NiOEP molecules on the surface to the total number of porphyrin molecules is defined either as Θ_{NiOEP}, or just as Θ_N for brevity in later equations. X_{NiOEP} (or X_N) is the ratio of molar concentration of NiOEP to the total molar concentration of both CoEOP and NiOEP in solution. Using these variables, the adsorption isotherm at 25 °C was obtained and plotted in Figure 3. Note that Θ_{NiOEP} and X_{NiOEP} are essentially equal suggesting that there might be a simple ideal equilibrium between surface and solution with the free energies of CoOEP and NiOEP being the same in each phase. This interpretation is wrong.

Our first indication that this was not an equilibrium system at 25 °C came as we counted molecules in sequential STM images. For example, images (Figure 4) taken at t, t + 150 s, and t + 300 s are shown with two points of relative reference marked. The red circle surrounds a vertical dimer and the white circle identifies a vacancy in the monolayer. Taking these two reference points, it is very clear that no CoOEP molecule moves on or off the surface in the full time frame of the experiment. In viewing all of our data taken at 25 °C, at many concentrations, and at different times, we never saw any indication of any MOEP molecule leaving a monolayer once it was formed. Experiments were then conducted with the sample heated to various temperatures and image at those temperatures. Representative images for 25 °C, 50 °C, and 70 °C are shown in Figure 5. Over the entire temperature range, all the images could be described by $\Theta_N = 0.82 \pm 0.03$. It should be noted that $X_N = 0.79 \pm 0.04$ for this data set.

Clearly, in the temperature range up to 70 °C, the adlayer is either not in chemical equilibrium with the solution, or both the ΔG and ΔS of adsorption (and thus the ΔH) are all the same for CoOEP and for NiOEP. This latter possibility seems unlikely, and the fact that no change is seen in the detailed positions of molecules in the adsorbed layer with time at 25 through 70 °C also argues against an equilibrium model. To be certain, however, we modified our experimental procedure to allow us to observe the rates of desorption of the MOEP species and to perform our measurements reliably on a time scale much longer than it is possible to image one particular region on a surface.

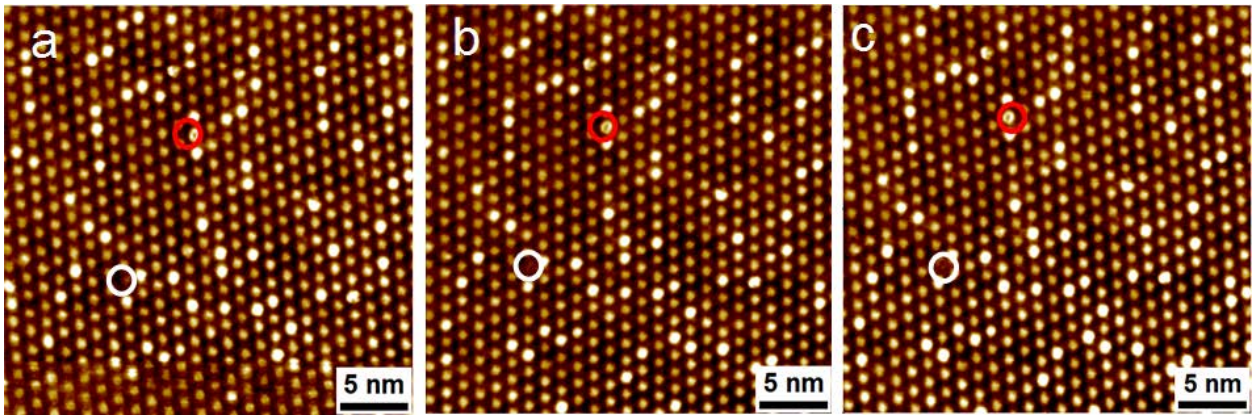

Figure 4: Sequential STM images taken from a monolayer formed from contact with a solution having $X_N = 0.79$. Images are taken about 2.5 minutes apart in time. Set point was -0.7 V and 20 pA.

A dense monolayer of a single MOEP was first created. Then, the solution above it was changed to a mixture of both CoOEP and NiOEP with the species NOT present in the original monolayer in excess in solution. If any exchange occurs between solution and surface, it will become apparent because of the change in molecular contrast. Because we are looking for any change on a statistical basis, there is no need to monitor the same area with time and long periods of time can be used. An example of the low temperature results is given in Figure 6 where some of the 25°C images are shown. At 25 °C it is very clear that, even on a time scale of hours, no exchange is occurring and therefore no desorption is occurring from the surface once a

monolayer forms. Similar results were obtained at temperatures approaching 100 °C. Obvious exchange in a one hour period was not seen until about 120 °C. On the other end of the time scale, following a pure solution with a mixture after only a few seconds exposure yielded exactly the same results – a single species monolayer. Thus, the monolayer is formed in about 1-10 seconds

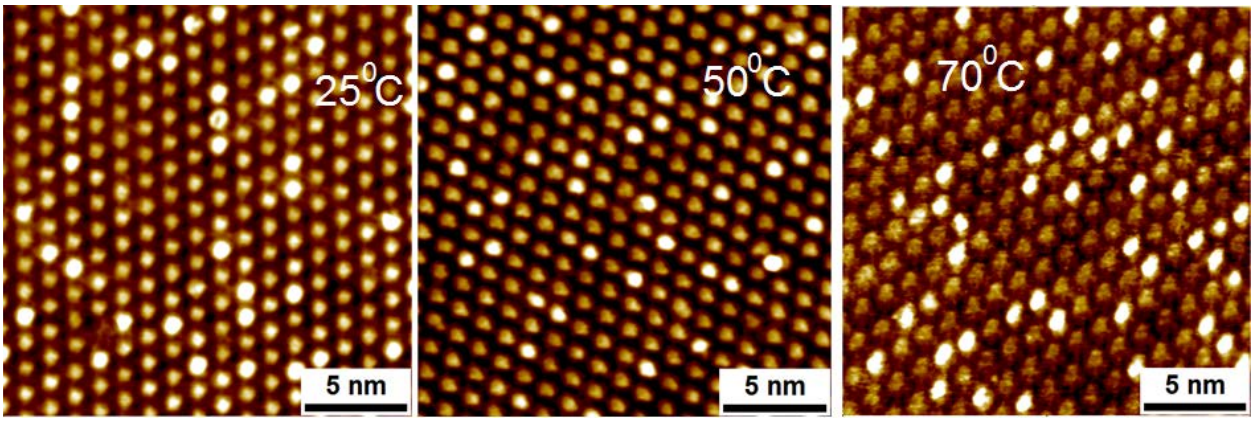

Figure 5: Constant current STM images taken from monolayers formed from contact with a solution having $X_N = 0.79$ at different temperatures. These are in situ images acquired at the temperatures indicated. Set point was -0.7 V and 20 pA.

At 135°C the rate of desorption was such that significant changes in the monolayer composition could be seen in about 2 hours. We therefore focused on this temperature in order to determine the rate of desorption. We initially thought the measurements would be symmetrical. That is, we thought that the CoOEP desorption in the presence of excess NiOEP would be qualitatively similar to the desorption of NiOEP in the presence of CoOEP. This was not correct. As can be seen in Figure 7, when NiOEP is initially replaced by CoOEP at 135 °C, the nickel species preferentially desorbs from the step edges and along reconstruction lines. On the other hand, at the same temperature, the CoOEP desorption does not appear to be site specific. The remainder of this paper will focus on the simpler NiOEP desorption problem and leave analysis of the CoOEP desorption for a subsequent study.

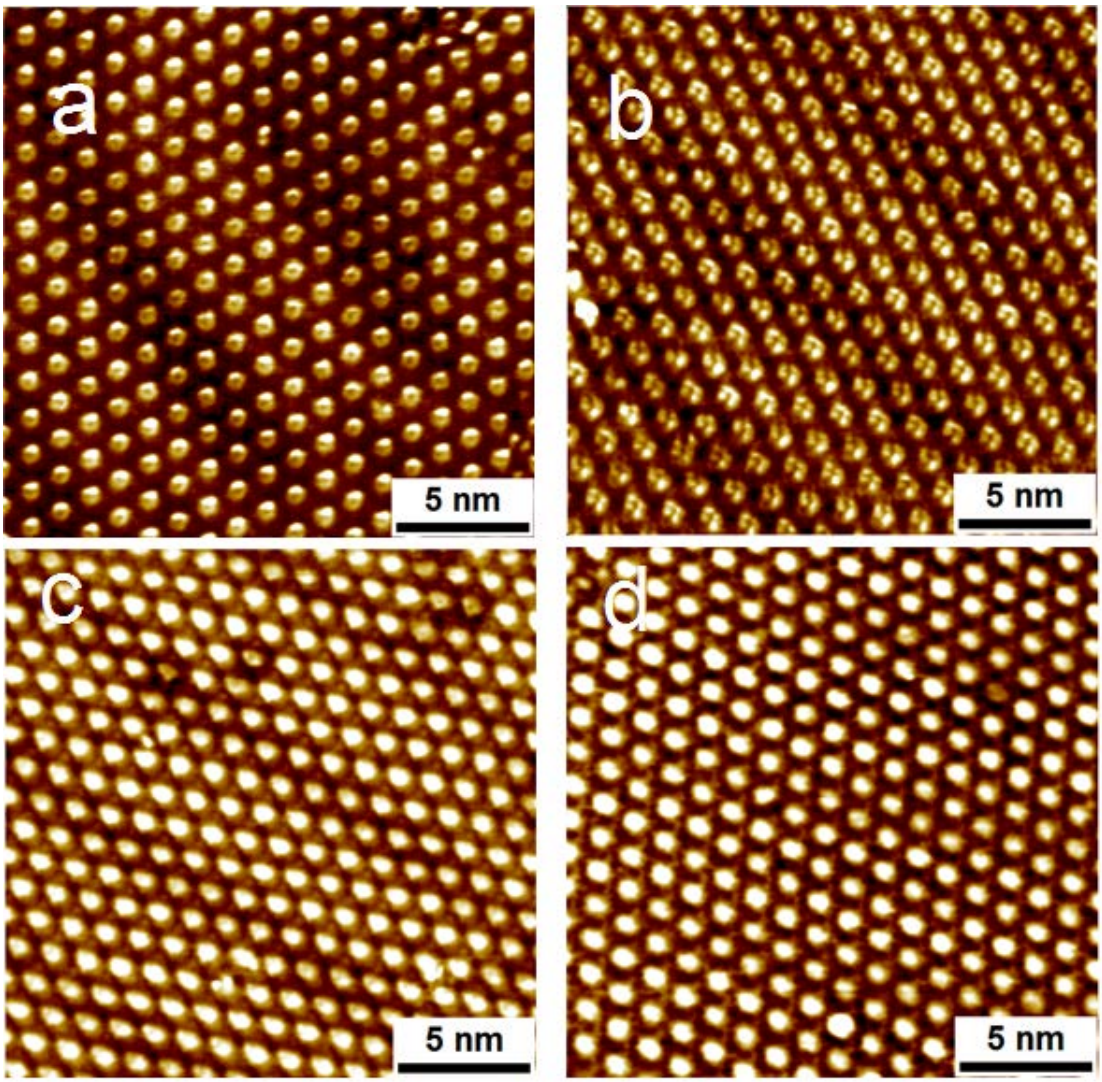

Figure 6: STM images obtained at 25 °C. a) Solution of NiOEP in phenyloctane in equilibrium with Au(111); b) monolayer from a exposed to a solution having $X_N = 0.31$ for a period of 2 hours. c) Solution of CoOEP in phenyloctane in equilibrium with Au(111); b) monolayer from c exposed to a solution having $X_N = 0.88$ for a period of 24 hours. Set point was -0.70 V sample bias and 20 pA tunneling current.

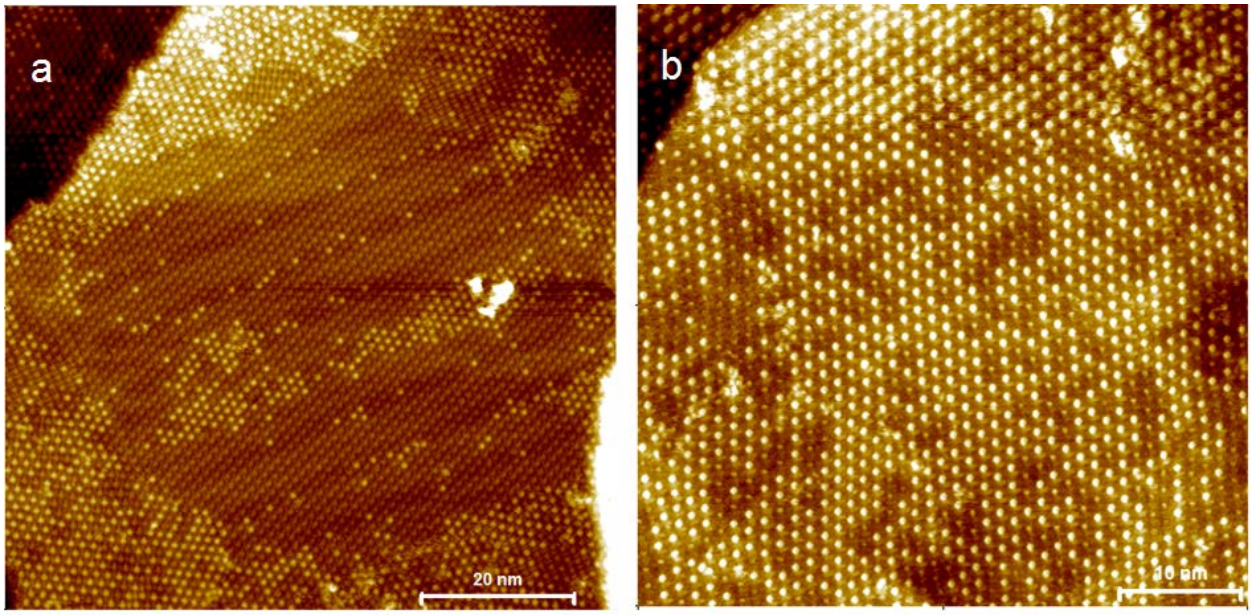

Figure 7: STM image of the MOEP in phenyloctane / Au(111) interface after 30 minutes exposure to a mixed composition solution at 135°C. a) Initially full monolayer of NiOEP exposed to $X_N = 0.31$ solution for 60 min. b) Initially full monolayer of CoOEP exposed to $X_N = 0.88$ solution for 90 min. [CoOEP] = 1.4×10^{-5} M and [NiOEP] = 9.7×10^{-5} M. Set point was -0.70 V sample bias and 20 pA.

Monolayer samples of CoOEP were prepared and imaged by STM. They were then exposed to a solution of NiOEP and CoOEP in phenyloctane ($X_N = 0.88$) at 135°C for varying lengths of time. After each time interval the sample was cooled quickly to room temperature and repeatedly measured in order to obtain statistically significant values for the relative NiOEP coverage. Figure 8 displays the results of measurements ranging from zero to 180 minutes. We would expect to see the greatest systematic error associated with insufficient time at temperature in the short time sample, and we do see such a trend.

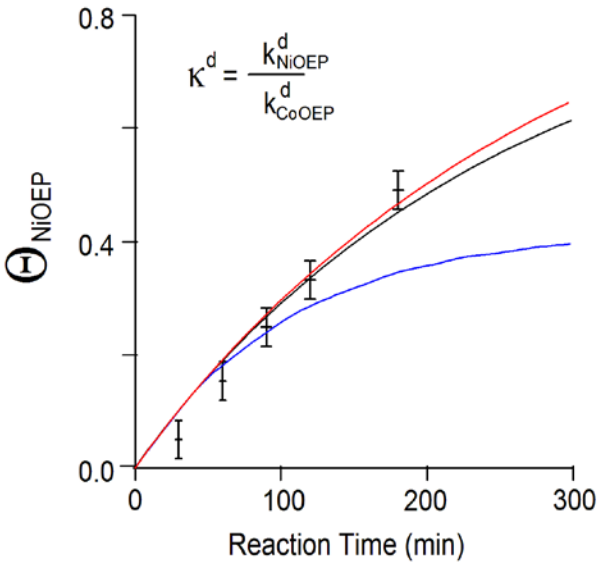

Figure 8: NiOEP coverage with reaction time at 135°C. Red : κ^d=0.1, k_C^d=0.004/min; black: κ^d=1.0; k_C^d=0.004/min blue: κ^d= 10, k_C^d=0.0035/min

What is immediately apparent in Figure 8, is that even after 3 hours of exposure to a solution at 135°C, $\Theta_{NiOEP}/ X_{NiOEP}$ is only about 0.5. Thus, the desorption of CoOEP from Au(111) is a very sluggish process even at this high temperature. In order to make quantitative statements about the rates, a model is required. In the next section we introduce such a model.

It is clear from the data presented above that the rate of formation of a monolayer is many orders of magnitude faster than the rate of desorption. Thus, our model will be based on the severability of these two problems. Let us first define the probability that a particular vacant site in the monolayer will be filled by a NiOEP from solution, call this P_N. Define it as:

$$P_N = \left[\frac{\frac{d\theta_N}{dt}}{\frac{d\theta_N}{dt} + \frac{d\theta_C}{dt}} \right] \qquad \text{(eq 1)}$$

Where the measurements are made during the formation phase of the monolayer and reflect the high speed adsorption kinetics.

$\frac{d\theta_N}{dt} = k_N^a X_N M(1-\theta)$ where k_N^a is the rate constant for the adsorption of NiOEP, X_N is the mole fraction of NiOEP in solution, M is the total molarity of porphyrins in the solution, and θ_N is the fractional coverage by NiOEP. Similarly $\frac{d\theta_C}{dt} = k_C^a X_C M(1-\theta)$, for CoOEP, and

$\theta = \theta_N + \theta_C$. Combining these, we find that $\theta = (1 - e^{-\bar{k}t})$ where $\bar{k} = \left(k_N^a X_N + k_C^a X_C\right) = k_N^a X_N + k_C^a (1 - X_N)$. Substituting this back into the rate equation of NiOEP adsorption, we find that

$$\theta_N = (1 - e^{-\bar{k}Mt})\left(\frac{k_N^a X_N}{\bar{k}}\right) \qquad \text{(eq 2)}$$

Let us digress for a moment to consider the application of Equation 2 to the adsorption isotherm shown in Figure 3. Equation 2 can be used to predict the relative coverage observed at low temperatures where the desorption rate is very slow since at long times, $\theta_N = \left(\frac{k_N^a X_N}{\bar{k}}\right)$. Note that at low temperatures and for a complete monolayer, θ_N depends only upon the ratio of the adsorption rates and upon the mole fraction in solution. We have applied this equation to the data at 25°C in order to determine an envelope in which the rates of adsorption must lie. Defining κ^a as the ratio of the adsorption rates, and observing the plots in Figure 3, ***it is clear that the rates of adsorption of NiOEP and of CoOEP are within 40% of each other.*** It is important to take a moment here and to realize that the above rates are the effective overall rates for formation of a monolayer. These need not be the correct rates for early stages of adsorption where there is little, if any, intermolecular interaction.

Returning to our original problem, we can combine the above results to find that:

$$P_N = \left[\frac{\frac{d\theta_N}{dt}}{\frac{d\theta_N}{dt} + \frac{d\theta_C}{dt}}\right] = \frac{k_N^a X_N}{k_C^a X_C + k_N^a X_N} = \frac{k_N^a X_N}{\bar{k}} \qquad \text{(eq 3)}$$

We now turn to the much slower desorption process. The rate of appearance of NiOEP on a full monolayer containing both Ni and Co sites will be equal to : (the rate of disappearance of Co times the probability that the site will be filled by Ni) – (the rate of disappearance of Ni times the probability that it will be replaced by Co). Thus:

$$\frac{d\vartheta_N}{dt} = k_C^d(1-\vartheta_N)P_N - k_N^d\vartheta_N(1-P_N) = k_C^d P_N + \vartheta_N(k_N^d P_N - k_C^d P_N - k_N^d) \qquad \text{(eq 4)}$$

Assuming that the rates of adsorption for NiOEP and CoOEP are the same (a good assumption based on Figure 3), $P_N = X_N$, and equation 4 can be written as $\frac{d\vartheta_N}{dt} = k_C^d X_N(1+a\vartheta_N)$, where $a = \left[(\frac{k_N^d}{k_C^d X_N})(X_N - 1)\right] - 1$. Integrating from time 0 where $\Theta_N =$ 0 to time t where Θ_N takes on its observed value $\int_0^{\Theta_N} \frac{d\vartheta_N}{1+a\vartheta_N} = k_C^d X_N t$. The result of this integration is:

$$\Theta_N(t) = (\frac{1}{b})(1-e^{-bk_C^d X_N t}) = \frac{k_C^d X_N}{k_C^d X_N + k_N^d(1-X_N)}\left[1-e^{-bX_N k_C^d t}\right] \qquad \text{(eq 5)}$$

And $$b = \left\{1+\left[(1-X_N)\left(\frac{k_N^d}{k_C^d X_N}\right)\right]\right\} \qquad \text{(eq 6)}$$

We have used equations 5 and 6 to estimate the possible values of k_C^d and κ^d. Given the value of X_N=0.88 used in the experiment, curves for θ(t) are plotted in Figure 8. Based on this figure, it is clear that the desorption rate for CoOEP must be close to 0.004 /min or $6.7\text{x}10^{-5}$ /s.

Comparing the blue trace to the data in Figure 8, it is clear that that the desorption rate for NiOEP is not 10 times faster than that for CoOEP. On the other hand, the NiOEP desorption rate might be very much slower than for CoOEP. A much more precise evaluation of k_N^d can be extracted from measurements made at other values of X_N, and those experiments are underway.

It is valuable to contrast the size of k^d for these large molecules bound by weak forces to that for a smaller molecule attached by a covalent bond. Karpovich and Blanchard determined that the desorption rate for 1-octanethiol from Au(111) in n-hexane at 25°C was 25./min. [49] This is over 6,000 times faster than for CoOEP desorbing from gold at 135°C! Thiols bonded to gold are often discussed in terms of surface modifying agents. The fact that porphyrins are so much more resistant to solvent removal should lay to rest any expectation that the solution solid interface is always fragile.

Finally, we report on the molecular spacing observed for the pure CoOEP and NiOEP monolayers. For CoOEP, A = 1.42±0.02 nm, B= 1.32±0.02 nm, and α = 57º±1º. For NiOEP A = 1.41±0.01 nm, B= 1.33±0.01 nm, and α = 58º±1º. We note that because we could not resolve the individual ethyl groups it was impossible to determine the true unit cell parameters. The values given here assume a single molecule per unit cell, but this may be incorrect since it is known from high resolution UHV STM studies that NiOEP vapor deposited on Au(111) prefers a cell with 2 molecules slightly rotated relative to each other.

Given the precision of the above measured molecular spacing, we must conclude that the CoOEP and NiOEP occupy identical environments and volume in the monolayer. Thus, it is very likely that the adsorbate-adsorbate interactions are nearly identical and differences in behavior must arise from adsorbate-substrate and adsorbate solvent differences. Because the solubilities are similar (3.9×10^{-4} M and 5.4×10^{-4} M), it also seems unlikely that adsorbate-solvent

interactions are significantly different. Thus, differences in desorption may come primarily from adsorbate-gold interactions.

CONCLUSIONS

For the first time scanning tunneling microscopy has been used to study the kinetics of molecular desorption at the solid-solution interface. The relative coverage of a binary mixture of porphyrins adsorbed from phenyloctane onto Au at room temperature is entirely kinetically controlled. For solutions of the order of 100 μM in NiOEP or CoOEP, a dense monolayer is formed within seconds. Contrary to conventional thinking, non-covalent adsorption can lead to exceedingly strong molecular binding such that solution-surface equilibration is extremely slow even above 100°C. The rate of desorption of CoOEP from a Au(111) surface in contact with phenyloctane solution at 135°C is only 6.7×10^{-5} /s and orders of magnitude slower than for a covalently bound thiol at 25°C. The structure of NiOEP and CoOEP monolayers are essentially identical and the molecular spacing for both can be described by A = 1.42±0.02 nm, B= 1.32±0.02 nm, and α = 57º±2º. NiOEP appears to desorb at different rates from step edges, reconstruction lines, and terraces. The CoOEP desorption rate seems to be more spatially uniform. We are in the process of extending these measurements to fully determine both the adsorption and desorption rate constants and the thermodynamic equilibrium values at high temperatures where equilibration occurs in finite times. We are also pursuing these studies on HOPG.

ACKNOWLEDGEMENTS

This material is based upon work supported by the National Science Foundation under grants CHE-1112156, and CHE-1058435.

REFERENCES

[1] Bourikas, K.; Kordulis, C.; Lycourghiotis, A. *Catal. Rev.: Sci. Engin.* **2006**, *48*, 363-444.

[2] Yerushalmi-Rozen, R.; Klein, J.; Fetter, L. J. Science **1994**, *263*, 793-795.

[3] Zhang, Y.; Wen, S. *Tribology Trans*. **2002**, *45*, 135-144.

[4] Lee, S.; Muller, M.; Rezwan, K.; Spencer, N. D. *Langmuir* **2005**, *21*, 8344-8353.

[5] Allen, C,M,; Drauglis, E. *Wear* **1969**, *14*, 363-384.

[6] Trentler, T. J.; Hickman, K. M.; Goel, S. C.; Viano, A. M.; Gibbons, P. C.; Buhro, W. E. *Science* **1995**, *270*, 1791-1794.

[7] Reddy, M. M.; Gaillard, W. D. *J. Colloid Interf. Sci*. **1981**, *80*, 171-178.

[8] Mann, S.; Archibald, D. D.; Didymus, J. M.; Douglas, T.; Heywood, B. R.; Meldrum, F.C.; Reeves, N. J. *Science* **1993**, *261,* 1286-1292.

[9] Pawlowski, N. E.; Johnson, L. E.; Lauw, H. P.; Shields, J. P.; Rehman, Z. *U. S. Patent 5,626,655* **1997**.

[10] Street, R. A.; Wong, W. S.; Ready, S. E.; Chabinyc, M. L.; Arias, A. C.; Limb, S.; Salleo, A.; Lugan, R. *Materials Today* **2006**, *9*, 32-37.

[11] Cheng, K.; Yang, M.; Chiu, W.; Huang, C.; Chang, J.; Ying, T.; Yang, Y. *Macromolecular Rapid Comm.* **2005**, *26*, 247-264.

[12] Aernouts, T.; Aleksandrov, T.; Girotto, C.; Genoe, J.; Poortmans, J. *Applied Phys. Lett.* **2008**, *92*, 033306-1/3.

[13] Askadskaya, I.; Rabe, J. P. *Phys. Rev. Let.* **1992**, *69,* 1395-1398.

[14] Jahanbekam, A.; Vorpahl,S.; Mazur, Ursula; Hipps, K. W. *J. Phys. Chem. C* **2013**, *117,* 2914-2919.

[15] Walch, H.; Maier, A.; Heckl, W. M.; Lackinger, M. . *J. Phys. Chem. C* **2009,** *113,* 1014–1019.

[16] Ramachandran, G. K.; Hopson, J. T.; Rawlett, A. M.; Nagahara, L. A.; Primak, A.; Lindsay, S. M. *Science* **2003**, *300*, 1413-1416.

[17] Marie, C.; Silly, F.; Tortech, L.; Mullen, K.; Fichou, D. *ACS Nano* **2010**, *4*, 1288-1292.

[18] Giesen, M.; Baier, S. *Journal of Physics: Condensed Matter* **2001,** *13*, 5009-5026.

[19] Gutzler, R.; Sirtl, T.; Dienstmaier, J. F.; Mahata, K.; Heckl, W. M.; Schmittel, M.; Lackinger, M. *J. Am. Chem. Soc.* **2010**, *132*, 5084–5090.

[20] Friesen, B.A.; Bhattarai, A.; Hipps, K. W.; Mazur, U. *J. Am. Chem. Soc.* **2012**, 134, 14897-14904.

[21] Schull, G.; Douillard, L.; Fiorini-Debuisschert, C.; Charra, F.; Mathevet, F.; Kreher, D.; Attias, A. *Adv. Mater.* **2006**, *18*, 2954-57

[22] MacLeod, Jennifer M.; Rosei, F. *Austr. J. Chem.* **2011**, *64*, 1297-1298.

[23] English, W. A.; Hipps, K. W. *J. Phys. Chem. C* **2008,** *112,* 2026-2031

[24] Dretschkow, T.; Wandlowski, T.; Wandelt, K.; Thurgate, S. (Eds.): Structural Transitions in Organic Adlayers – A Molecular View. Solid–Liquid Interfaces, Topics Appl. Phys. **2003,** *85*, 259–324. Springer-Verlag Berlin Heidelberg.

[25] Jeong, Y.; Han, Jin W.; Lee, C.; Noh, J. *Bull. Korean Chem. Soc.* **2008**, *29*, 1105-1106.

[26] Yoshimoto, Soichiro; Honda, Yosuke; Ito, Osamu; Itaya, Kingo. *J. Amer. Chem. Soc.* **2008**, *130*, 1085-1092.

[27] Yoshimoto, S.; Yokoo, N.; Fukuda, T.; Kobayashi, N.; Itaya, K. *Chem. Comm.* **2006**, 500-502.

[28] Wan, L.; Shundo, S.; Inukai, J.; Itaya, K. *Langmuir* **2000**, *16*, 2164-2168.

[29] Hipps, K. W.; Lu, X.; Wang, X. D.; Mazur, U. *J. Phys. Chem.* **1996,** *100*, 11207-11210.

[30] Lu, W.; Hipps, K. W. *J Phys. Chem. B*, **1997** ,*101*, 5391-5396.

[31] Takami, T.; Carrizales, C.; Hipps, K. W. *Surf. Sci.* **2009,** *603*, 3201-3204.

[32] Barlow, D.; Hipps, K. W. *J. Phys. Chem B*, **2000**, *104*, 5993-6000.

[33] Scudiero, L.; Barlow, D. E.; Hipps, K. W. *J. Phys. Chem. B* **2002**, *106*, 996-1003.

[34] Hipps, K. W.; Scudiero, L.; Barlow, D. E. *J. Amer. Chem. Soc.* **2002,** *124*, 2126-27.

[35] Barlow, D.E.; Scudiero, L.; Hipps, K. W. *Langmuir* **2004**, *20*, 4413-21.

[36] Yoshimoto, S.; Tada, A.; Suto, K.; Yau, S.; Itaya, K. *Langmuir* **2004**, *20*, 3159-3165.

[37] Yoshimoto, S.; Higa, N.; Itaya, K. *J. Amer. Chem. Soc.* **2004**, *126*, 8540-8545.

[38] Yoshimoto, S.; Inukai, J.; Tada, A.; Abe, T.; Morimoto, T.; Osuka, A. Furuta, H.; Itaya, K. *J. Phys. Chem. B* 2004, *108,* 1948-1954.

[39] Soichiro, Y.; Sato, K.; Sugawara, S.; Chen, Y.; Ito, O,; Sawaguchi, T.; Niwa, O.; Itaya, K. *Langmuir* **2007**, *23*, 809-816.

[40] Miyake, Y.; Tanaka, H.; Ogawa, T. *Coll. Surf. A* **2008**, *313-314*, 230-233.

[41] Ogunrinde, A.; Hipps, K. W.; Scudiero, L. *Langmuir;* **2006,** *22*, 5697-5701.

[42] Mazur, U.; Hipps, K. W.; Riechers, S. L. *Journal of Physical Chemistry C* **2008**, *112*, 20347-20356.

[43] Otsuki, J.; Seki, E.; Taguchi, T.; Asakawa, M.; Miyake, K. *Chem. Lett.* **2007**, *36*, 740-741.

[44] Nakamura, M.; Imai, R.; Hoshi, N.; Sakata, O. *Surf. Sci.* **2012,** *13*, 1844-1852.

[45] Ikeda, T.; Asakawa, M.; Goto, M.; Miyake, K.; Ishida, T; Shimizu, T. *Langmuir* **2004**, *20*, 5454-5459.

[46] Otsuki, J.; Kawaguchi, S.; Yamakawa, T.; Asakawa, M.; Miyake, K. *Langmuir* **2006**, *22*, 5708-5715.

[47] Ikeda, T.; Asakawa, M.; Miyake, K.; Goto, M; Shimizu, T. *Langmuir* **2008**, *24*, 12877-12882.

[48] Scudiero, L.; Darlow, D. E.; Mazur, U.; Hipps, K. W. *J. Am. Chem. Soc.* **2001**, *123*, 4073-4080.

[49] Karpovich, D. S.; Blanchard, G. J. *Langmuir* **1994,** *10*, 3315-3322.

TOC GRAPHIC